Commissioning Report for the ATCA L/S Receiver Upgrade Project

N. M. McClure-Griffiths, J. B. Stevens, & S. P. O'Sullivan

8 June 2011

1 Introduction

The original Australia Telescope Compact Array (ATCA) operated over two separate narrow bands covering 1.25 - 1.8 GHz (20 cm) and 2.2 - 2.5 GHz (13 cm). The maximum instantaneous bandwidth in either band was 128 MHz per IF, limited by the correlator, although the feedhorns and dual linear Ortho Mode Transducers (OMTs) themselves were capable of receiving the full 550 MHz and 300 MHz, respectively. In 2004, in preparation for the Compact Array Broadband Backend (CABB) upgrade we proposed to upgrade the 20/13 cm receiver systems to take advantage of the 2 GHz correlator bandwidth available in CABB, and to simultaneously fix a long-standing problem with the polarization performance of the receivers in the 13 cm band. The original science case and project proposal was submitted in September 2004, with updates to the science case in November 2004 and September 2006. We proposed to remove the band separating diplexers, replace the individual narrow-band LNAs with wide bandwidth LNAs covering 1.1 - 3 GHz and to modify the OMTs to improve the polarization performance

1.1 Scientific Specifications

The L/S & C/X upgrade project was motivated by the desire to provide more continuously sampled frequency coverage from 1 to 12 GHz, starting with the 1-3 GHz band; improve the continuum sensitivity; and improve the polarization response at 13 cm. As CABB progressed we also became aware that the L/S upgrade was required in order to retain the capability of simultaneously observing in the 20 cm and 13 cm bands. The three main scientific projects for L/S proposed in the science case were: deep continuum surveys, spectro-polarimetric studies of the Milky Way and other galaxies, and Lunar Cherenkov radiation.

It is obvious that deep continuum observations would be dramatically improved by increasing the available bandwidth at 20 and 13 cm. Our expectation was that simply increasing the instantaneous frequency coverage to the bandwidth of the CABB would provide a factor of $\sim$4 increase in continuum sensitivity and reduce the observing time for deep continuum observations by more than a factor of 10. This was expected to have dramatic implications for sensitivity limited continuum observations, particularly deep fields and rapid source follow-ups. To enable deep continuum science the requirements were: as large an instantaneous bandwidth as possible and no increase in system temperature over original receivers.

Spectro-polarimetric studies of the Milky Way and other galaxies in the 20 and 13 cm bands prior to the upgrade were limited both by the available wavelength coverage and a problem with the off-axis polarization at 13cm. Since the construction of the ATCA it was known that the polarized beam at 13cm was asymmetric (Sault & Ehle 1996), which prevented high-precision wide-field polarimetry at 13cm. The problem, which was due to the ortho-mode-transducer (OMT), was to be fixed during the upgrade. Our expectations were that the excellent polarized beam shape at 20 cm would be replicated across the 1-3 GHz band, allowing wide-field spectro-polarimetric studies.

Recent work in spectro-polarimetric studies have made use of a new technique called Rotation Measure (RM) synthesis (Brentjens & de Bruyn 2005). RM synthesis is powerful analysis tool that provides a means of continuously dissecting the interstellar medium (ISM) along the line of sight. By resampling the data with wavelength squared, λ^2, and taking the Fourier transform of the complex Stokes vector as a function of λ^2 we can directly measure the polarized signal as a function of Faraday depth into the ISM. The key specifications in rotation measure synthesis, other than polarization purity across the field of view, are the shortest and longest wavelength observed, λ_{min} and λ_{max}; the total bandwidth in λ^2 space, $\Delta(\lambda^2) = \lambda^2_{max} - \lambda^2_{min}$; and the channel width, $\delta(\lambda^2)$. These determine the effective RM resolution, $\delta\phi \approx 2\sqrt{3}/\Delta(\lambda^2)$, the maximum RM detectable $\phi_{max} \approx \sqrt{3}/\delta\lambda^2$, and the largest detectable scale $\propto \lambda^{-2}_{min}$. Therefore, the main specifications for the upgrade were to achieve as large a $\Delta(\lambda^2)$ coverage and as low a λ_{min} as the receivers and RFI environment would allow.

The final scientific observations described in the science case were those of Lunar Cherenkov, which aims to detect radio emission from Cherenkov cascades from neutrino interactions with the Moon's surface. Dagkasamensky & Zheleneznykh (1992) estimate that these Cherenkov cascades should result in very brief (<microsecond), strong (4000 Jy at 1420 MHz) pulses which peak in the 1 - 3 GHz range. These brief pulses should be detectable by radio telescopes with sufficiently high time resolution. The ATCA primary beam at 20 cm is well matched to the moon size and detection Lunar Cherenkov radiation might be possible given sufficient time resolution. The time resolution achieved is limited by the maximum instantaneous bandwidth of the receiver: gigahertz bandwidths would enable nanosecond time resolution. The polarization of the detected emission can provide positional information about the detected pulses. The main technical requirements for this project were a large instantaneous bandwidth, preferably the covering full 1 - 3 GHz band and a flat polarimetric response across the band.

In summary, the scientific specifications of the upgrade were simply:

- Continuous frequency coverage from 1 to 3 GHz for the 20/13 cm feeds
- Polarization purity to $\sim$ 1-2% across the entire 20/13 cm band
- No system temperature increase at current observing frequencies
- Designs and mitigation techniques to reduce the impact of RFI (may include pre-amplification notch filters)

2 System Performance

The original OMTs were removed and re-installed as the first step in the upgrade process, followed by the installation of the upgraded broadband LNAs. A proof-of-concept receiver system was installed on the ATCA in November 2009, with upgrading of all ATCA 20/13 cm receivers carried out between June and December 2010. System tests were conducted as the upgraded receivers were installed with the first set of scientific broadband polarimetry observations conducted with the full suite of receivers in December 2010. Here we discuss the system performance, particularly the available bandwidth; system temperature; polarization purity, both on and off-axis; and total power beam shape.

2.1 System Temperature

System temperature measurements were conducted in June 2010 on the first upgraded receiver, CA02, and were analysed by J. Stevens. The measurements were made by placing a known hot load, $T_{hot} = 295.25$ K in front of the receiver and comparing to sky measurements, T_{sky}. Here we have assumed that the sky is a cold blackbody of 2.725 K (CMB). In practice this is not strictly correct, depending on position the Galactic continuum emission can dominate at the low end of the 1-3 GHz band, dropping with frequency with a synchrotron spectrum. The observations were made at positions at least 20°from the Galactic plane where the sky temperature at 1 GHz can be assumed to be less than ~ 10 K and even less at 3 GHz.

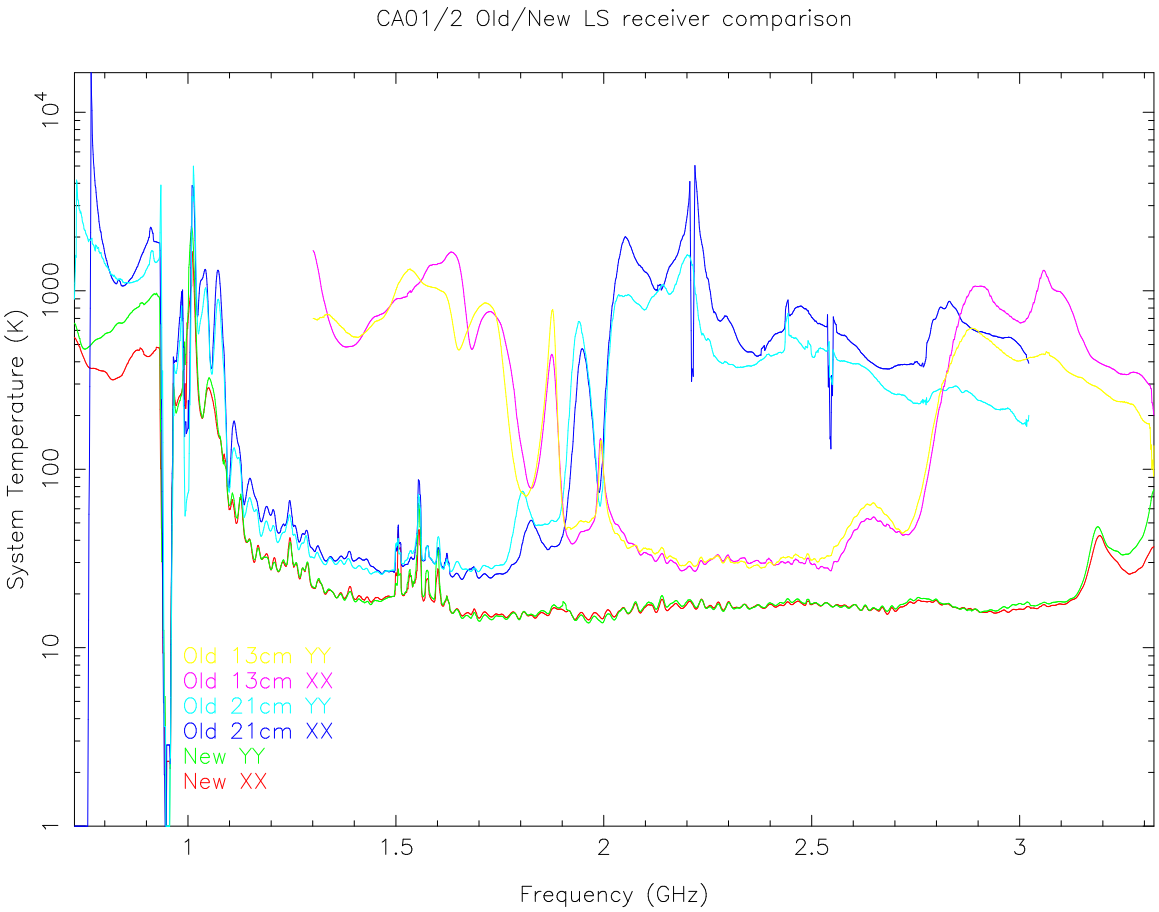

Figure 1: Comparison of 20 cm & 13 cm system temperatures with the old receiver on CA01 and the new 16 cm band system temperature on CA02. The coloured lines are as follows: old 13 cm YY (yellow), old 13 cm XX (purple), old 20 cm YY (cyan), old 20 cm XX (blue), new YY (green), new XX (red).

The system temperature is measured by comparing the hot and cold received powers:

$$P_{hot} = A(T_{sys} + T_{hot}), \tag{1}$$

$$P_{sky} = A(T_{sys} + T_{sky}), \tag{2}$$

to give:

$$T_{sys} = \frac{P_{hot}(T_{hot} - T_{sky})}{P_{hot} - P_{sky}} - T_{hot}. \tag{3}$$

Figure 1 shows a comparison of the system temperature of the old receiver on CA01 with the new 16cm band system on CA02. The difference is striking. The system temperature is very flat from from 1.3 - 3.1 GHz, with a slight rise between 1.1 and 1.3 GHz, owing both to the edge of the band and the prevailing interference below 1.1 GHz. Across most of the band the system temperature is ~ 20 K, almost a factor of two better than the lowest noise portions of the previous receiver system.

In terms of receiver performance, the band is usable from 1.1 - 3.1 GHz, with the recommended central frequency for observations of 2.1 GHz. At the low end of this frequency range RFI tends to affect observations. At the high frequency end, calibration is affected by the drop-off in the performance of the noise diode between 2.5 and 3 GHz.

2.2 Polarization Purity and Beam shape

The off-axis polarization at 13 cm has been known for many years to be asymmetric as a result of the OMT fin design. The effect of the fin design error produced spurious polarization features of greater than 10% beyond the beam half-power point. Sault & Ehle (1996) showed that observations of 1934-638 centred 420 arcsec away from the phase centre (60% of the half-power width), could produce Stokes Q, U, and V fluxes of 1.8%, 0.6% and 0.8% of the total intensity, even though the 1934-638 is known to be unpolarized to 0.03% in Stokes V (Rayner, Norris & Sault 2000). The spurious polarization effect increases as roughly the square of distance away from the beam centre up to at least the half-power point. Scans of sources at 13 cm showed that the primary beam shapes in the XX and YY correlations, as well as the total intensity were not symmetric. We expected that these effects will have been corrected by the OMT replacement.

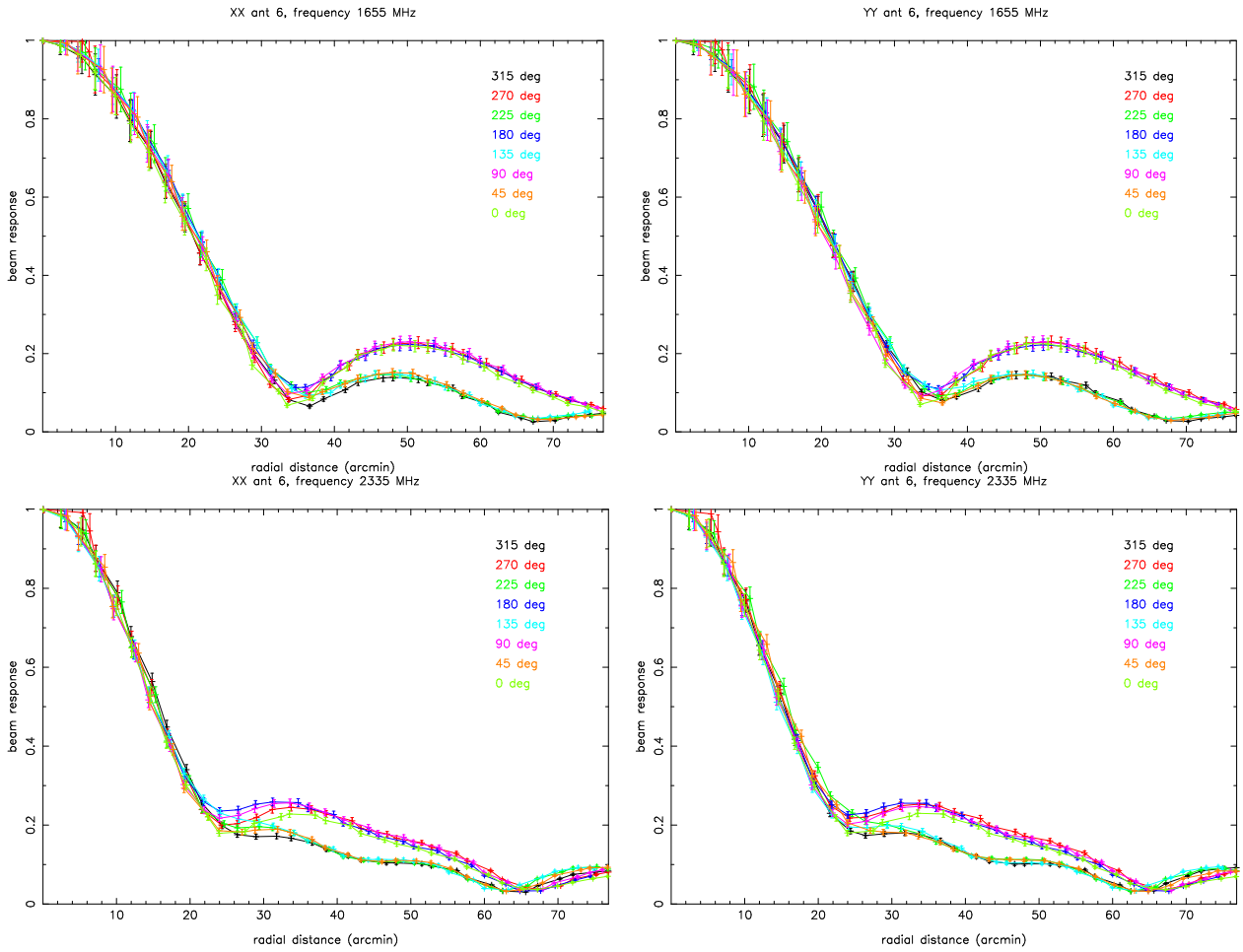

Figure 2: XX and YY beamshapes measured at various angles at 1.665GHz (top) and 2.335 GHz (bottom). The XX and YY main beams are very symmetric at both frequencies.

In August 2010, J. Stevens conducted measurements of the primary beam shape of the antennas containing the new receivers (CA02, CA03, CA04 & CA06). These observations were made using 0823-500, which is unpolarized to less than 0.15%, pointing CA02 directly on-source and moving the other antennas away in 2.4 arcmin increments up to 80 arcminutes. The measurements were repeated at eight angles with 45° increments, between 0° and 315°, measured from North in a clockwise direction.

Figure 2 shows measurements of the beam shape for XX and YY correlations at 1.665 and 2.335 GHz, showing that the beams are symmetric and similar at both frequencies. At the very high end of the band the symmetry begins to break down, but the effect is minimal.

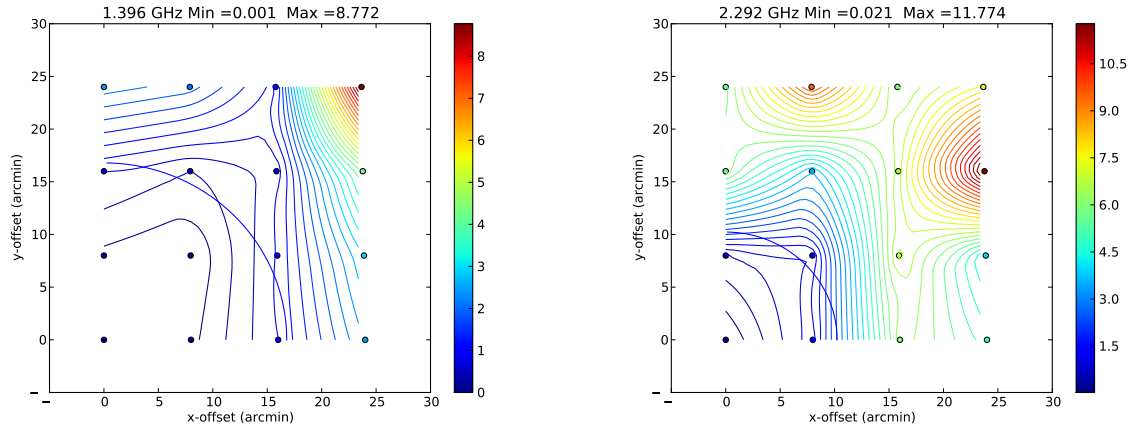

Figure 3: Interpolated percentage linear polarization measured off-source from observations of 1934-638 measured at 1.396 GHz (left) and 2.292 GHz (right). The colour of the contours represents the percentage linear polarization as given in the colour wedges. The filled circles mark the actual measurements.

To characterise the off-axis polarization we conducted pointed observations around PKS B1934-648, which is known to be unpolarized to $< 0.03\%$. We pointed in a 4 x 4 grid in increments of 8 arcmin away from 1934-638. The data were then analysed to determine the measured Stokes I, Q, & U flux at each point. Figure 3 shows the measured percentage linear polarization as a function of RA and Dec offset from 1934-638 at 1.396 GHz and 2.292 GHz. The half-power point in both maps is marked with the blue arc. The contours are scaled according to the colour wedge at the right of the images. These frequencies show the lowest off-axis linear polarization.

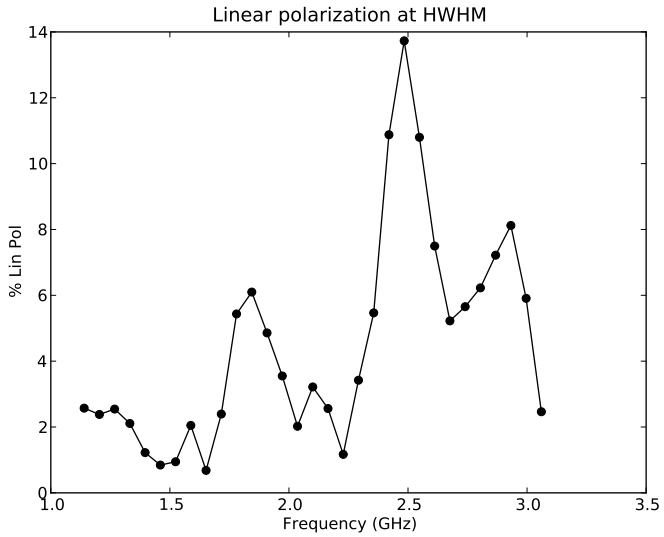

Figure 4: Percentage linear polarization at the half-power point as a function of frequency.

There is apparently variation in the magnitude of off-axis polarization with frequency. Figure 4 shows the estimated percentage linear polarization at the half-power point as a function of frequency. These values are measured at an angle of 45° from the North. The off-axis polarization is less than $\sim 3\%$ at 1.1-1.7 GHz and 2.1-2.3 GHz, but rises to more than 6% in between and again at frequencies > 2.6 GHz. The cause of these fluctuations is currently unknown but should be investigated more thoroughly. The increase beyond

2.6 GHz is possibly exacerbated by the small number of data points probing the inner beam and perhaps also calibration errors due to the fall-off in the performance of the noise diode above 2.5 GHz.

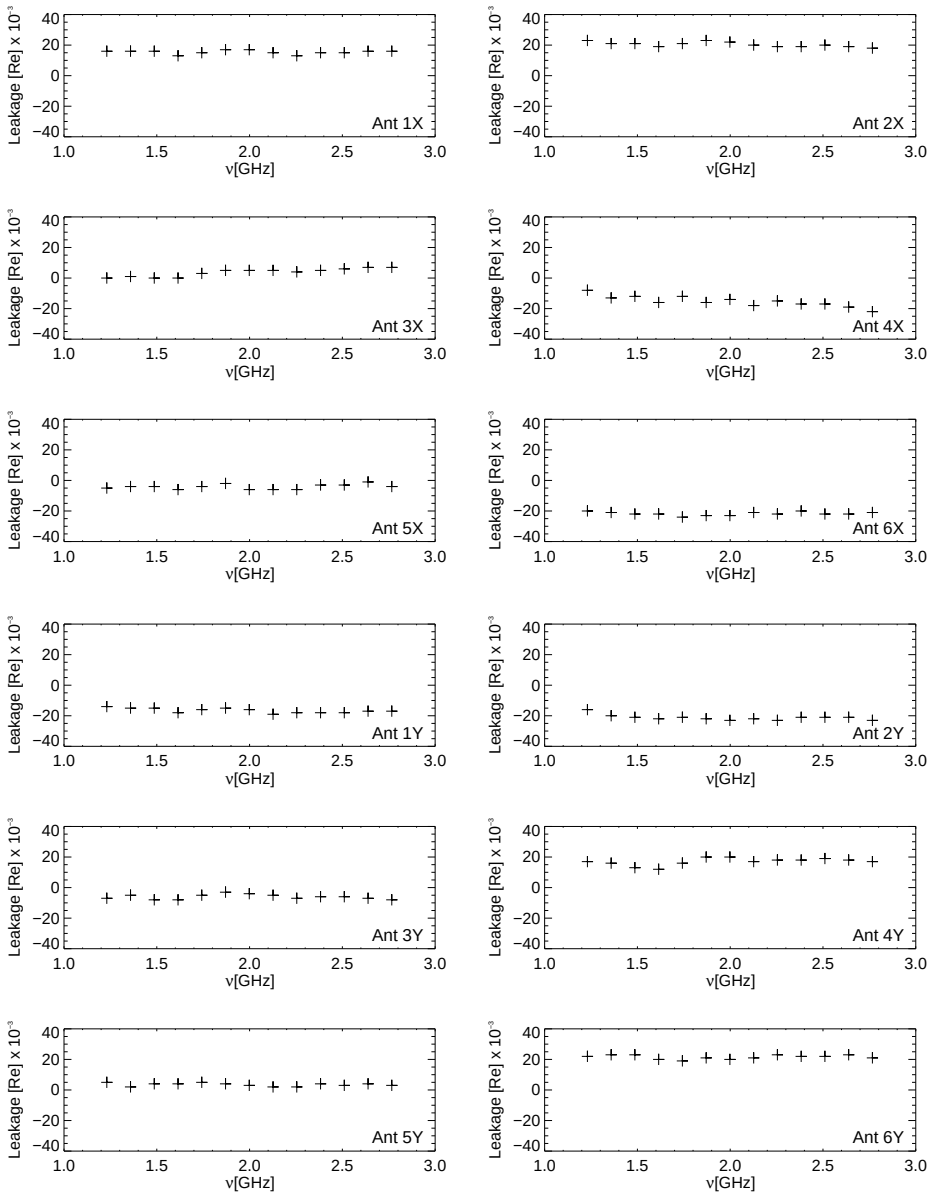

Figure 5: Plots of the real part polarization leakage vs frequency for the X (top) and Y (bottom) feeds. This provides information about the orthogonality of the feeds across the band. Note that the scale on the y-axis scale is in units of 10^{-3}.

The on-axis polarization purity (or leakage) across the band was explored through observations of several polarized point sources conducted in December 2010 as part of project C2437. The observations were split into 128 MHz chunks, each calibrated individually in Miriad. The leakage terms were examined across the whole band. The real part of the leakage term, plotted in Figure 5 for the X and Y feeds, respectively, probes the feed "misalignment", which gives information about how the feeds deviate from perfect orthogonality. The imaginary part of leakage term, plotted in Figure 6, probes the feed "ellipticity", giving information about any deviations from perfectly linear feeds. These figures show that the real part of the leakage is flat to better than 0.5% across the band and the imaginary part has maximum deviations of up to $\sim 2\%$ between 1.2 and 1.8 GHz.

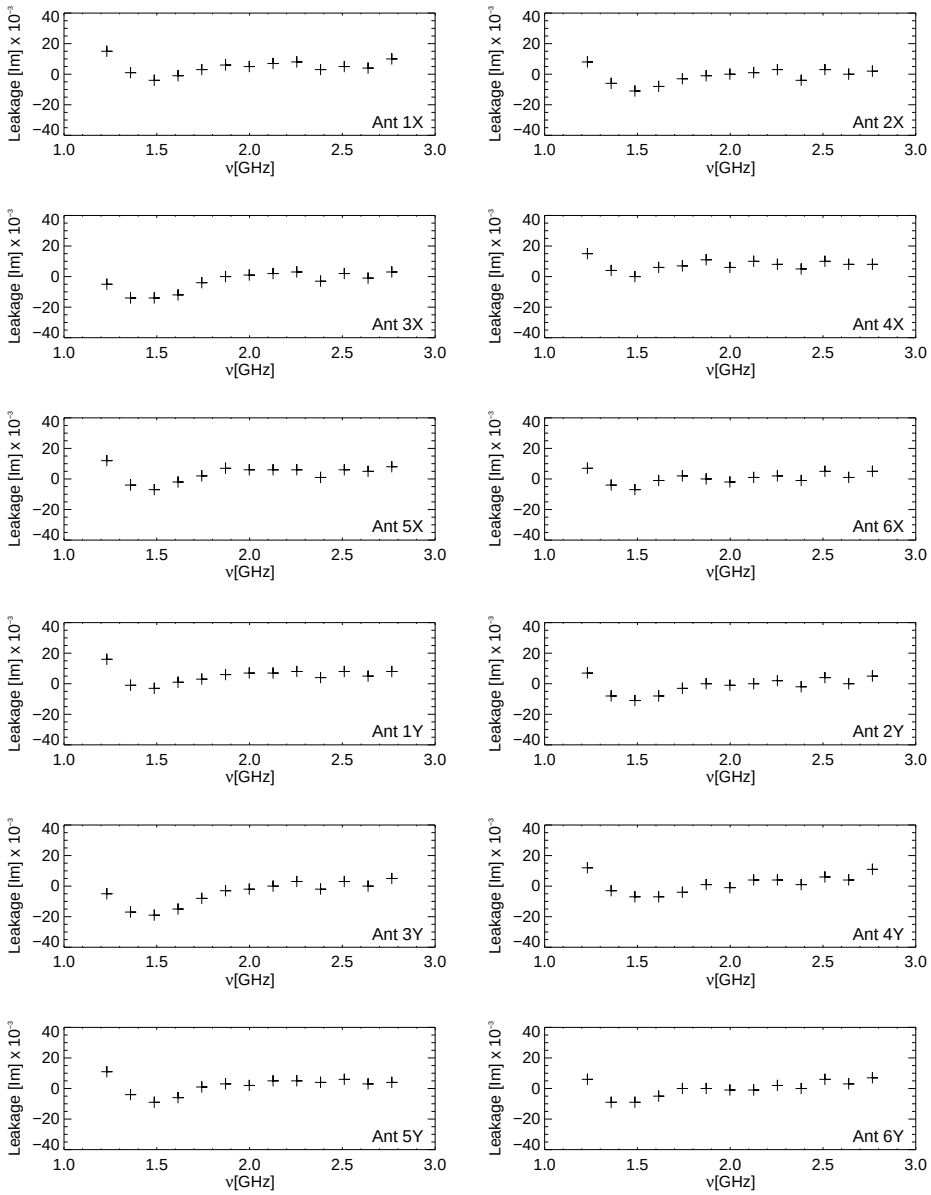

Figure 6: Plots of the imaginary part polarization leakage vs frequency for the X (top) and Y (bottom) feeds. The imaginary part of the leakage term provides information about the deviation from a perfectly linear feed. Note that the scale on the y-axis scale is in units of 10^{-3}.

Figure 7 shows measurements of the Stokes I beam shape at the eight angles and four different frequencies between 1.16 GHz and 3.025 GHz. The results show that the primary beam is very symmetric at all frequencies. The differences in the magnitude the sidelobes are a result of the feed-legs. Gaussian fits to the primary beam shape with angle show that the beams are on average symmetric to within 6%, with a maximum deviation of 12%. The difference between the sidelobe amplitudes at different angles is a result of the support legs. The power in the sidelobes is surprisingly large, especially at the higher frequencies and should be examined further.

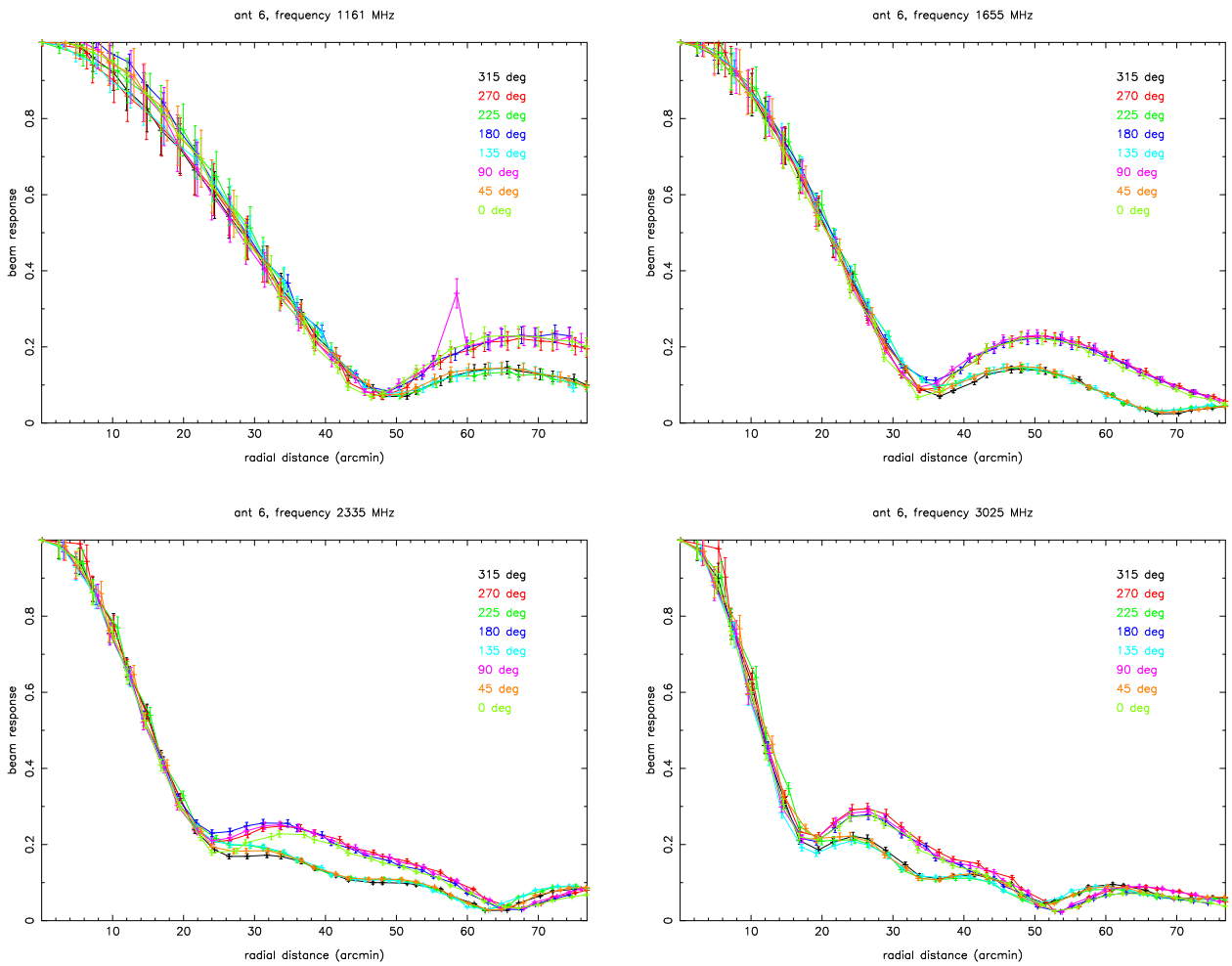

Figure 7: Stokes I beamshapes measured at various angles at 1.16 GHz, 1.665 GHz, 2.33 GHz and 3.025 GHz. The degree of symmetry of in the primary beam shape at high frequencies demonstrates that the new OMT has corrected the polarization problems.

3 Scientific Demonstration

Project C2437 (O'Sullivan), observed in December 2010 and January 2011, was one of the first projects scheduled on the array designed to take advantage of the new broadband system for high precision, broadband polarization observations. C2437 obtained 120 hours to image an area of $1.22\ \mathrm{deg}^2$ around 10 potential polarization calibrators. Each field was observed for $\sim$12 hours. The sources, which were primarily observed to characterise them as potential ASKAP polarization calibrators, have been analysed for their polarization properties vs frequency from 1.1 - 3.1 GHz. Absolute flux calibration and bandpass calibration was performed using 1934-638 and on-axis pointings of the calibrator were used for phase calibration. For calibration purposes the full band was split into chunks of 128 MHz in order to solve and correct for frequency dependent leakages. The calibrated data were then imaged in 10 MHz "channels", with an rms of $\sim 1\ \mathrm{mJy/Bm}$ for a 20 to 30 arcsec beam. Faraday rotation measure synthesis was performed on each pixel with detectable polarized flux.

Figure 8 shows a comparison of measurements of the polarization properties of the source B0454-810 versus frequency (or wavelength squared), as well as the RM spectrum for the new and old systems. The six panels on the top, labelled as *a*, show the results of the new broadband system, while the six panels below, labelled as *b*, show the equivalent data using the old 256 MHz bandwidth. Note particularly the

top, left panel of parts *a* and *b* which shows the rotation measure spectrum, i.e. the polarized intensity, p, as a function of Faraday depth, ϕ, or RM. The increased frequency coverage of the new system has greatly reduced the width of the RM spectrum and improved the RM resolution of the experiment. The RM measured for this source is $37.6 \pm 2.1 \ \mathrm{rad\ m^{-2}}$.

4 Summary

The ATCA L/S Upgrade to the new 16 cm receivers has been an outstanding success. The primary scientific specifications of correcting the 13 cm polarization properties, extending the centimetre band to take advantage of CABB and not increasing system temperature have all been achieved. The resulting system is a testament to excellent engineering, producing a receiver with system temperatures of order 20 K across a nearly 2 GHz band, and polarization purity on the order of $1 - 2\%$ across the band from 1.1 to 3 GHz. Scientific observations designed to take advantage of the broadband spectropolarimetry now available commenced almost immediately after the full receiver suite was installed and these are producing weird and wonderful results!

References

Brentjens, M. A. & de Bruyn, A. G. 2005, A&A, 441, 1217
Dagkesamansky, R. D., Zheleznykh, I. M. 1992, in Astrophysical Aspects of the Most Energetic Cosmic Rays. World Scientific, Singapore eds. M. Nagano & F. Takahara, p. 373
Rayner, D. P., Norris, R. P., & Sault, R. J. 2000, MNRAS, 319, 484
Reynolds, J. E. 1994, ATNF Technical Document Series, AT/39/3/040
Sault, R. J. & Ehle, M. 1996, ATNF Technical Document Series, AT39/3/088

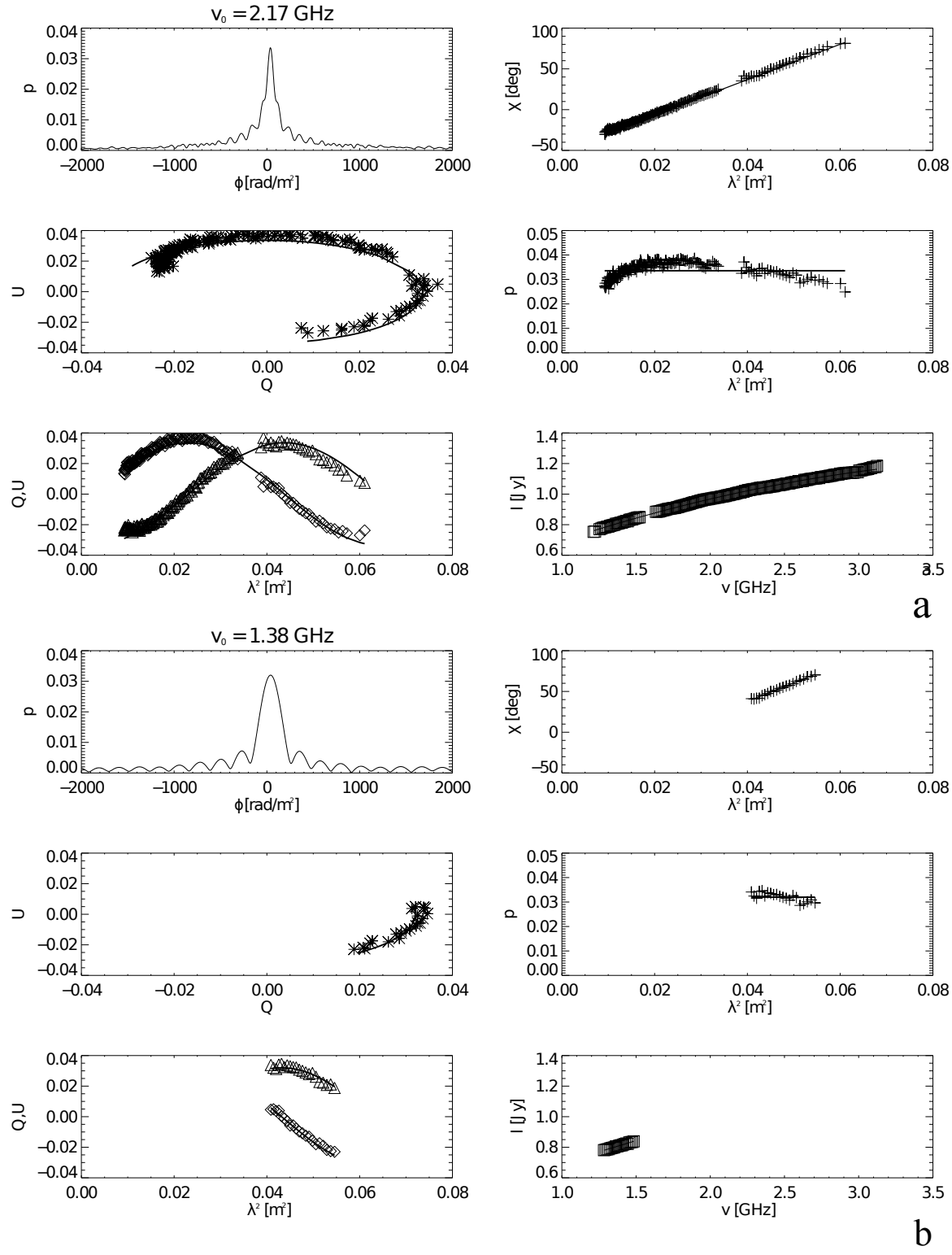

Figure 8: Polarization properties of B0454-810 using the new system (panel *a*) and the old system (panel *b*). Top left: Faraday depth vs. fractional polarization. Top right: Polarization angle vs. λ^2 (solid line represents a model of a single RM component extracted from the peak in the Faraday depth spectrum). Middle left: Q vs. U. Middle right: fractional polarization vs. λ^2 . Bottom left: Q and U vs. λ^2 . Bottom right: Total intensity vs. frequency (with a second-order polynomial fit).